

# Photoabsorption spectrum for OClO between 125 and 470 nm

S. Hubinger and J.B. Nee

*Department of Physics, National Central University, Chung-Li 32054, Taiwan, ROC*

Received 27 September 1993

Absolute absorbance cross sections for OClO were measured between 125 and 470 nm using a 0.5 m vacuum monochromator and a PMT detector. In all, 26 primary symmetric stretching bands and 24 combination bending and asymmetric stretching bands of the  $A^2A_2$  system were observed between 260 and 460 nm. Four additional band systems were also observed in the vacuum UV region between 125 and 190 nm. Cross sections were measured for three symmetric stretch C bands (183.08, 179.85 and 176.77 nm), nine symmetric stretch (162.66, 160.08, and 155.01 nm), asymmetric stretch (157.27 and 154.68 nm) and bending (161.38, 158.55, and 155.90 nm) D bands, seven bending E bands (156.75, 155.48, 154.30, 153.11, 151.99, 150.90, and 149.83 nm) and twenty-one F bands (144.29, 143.29, 142.17, 140.87, 139.78, 139.00, 138.00, 137.24, 136.22, 135.22, 134.38, 133.83, 133.20, 132.78, 132.06, 131.13, 130.61, 130.00, 128.51, 127.78, and 127.00 nm). In addition, a cross sectional minimum of  $4 \times 10^{-20}$  cm<sup>2</sup> molecule<sup>-1</sup> was found between the  $A^2A_2$  system and the C system near 248 nm. Finally, the observed C, D, E, and F states were analyzed in terms of Rydberg progressions leading to the first and second ionization potentials and allowed prediction of some relative energy levels in the ground state and in excited states.

## 1. Introduction

Symmetrical chlorine dioxide (OClO) is perhaps unique in both being a reactive radical intricately linked with the atmospheric ozone cycle and in being sufficiently stable (kinetically) and volatile to permit extensive investigation of its ground and excited states in terms of its rotational, vibrational and electronic states and decomposition paths. Microwave studies by Curl and others have shown that the ground electronic state is  $^2B_1$  and has a Cl-O bond radius of 1.471 Å and a O-Cl-O bond angle of 117.6° [1-7]. Ground state vibrational frequencies, as originally found by Coon and Ortiz, are symmetric stretch ( $\nu_1$ )=962.8 cm<sup>-1</sup>, bend ( $\nu_2$ )=455.4 cm<sup>-1</sup>, and asymmetric stretch ( $\nu_3$ )=1128.8 cm<sup>-1</sup> [8]. In addition, a large variety of high-resolution spectroscopic measurements have provided very precise data about the ground state potential energy surface in terms of equilibrium structure, force constants, and dipole moments [7-17]. Thus, the ground state electronic configuration is calculated to be as follows [18,19]:

$$X^2B_1: (\text{core}) (5a_1)^2(3b_2)^2(6a_1)^2(7a_1)^2 \\ (4b_2)^2(2b_1)^2(5b_2)^2(8a_1)^2(1a_2)^2(3b_1)^1.$$

Based on the ground state electronic configuration, three lower-level intervalence transfer excited states can be predicted. For the  $^2A_2$  excited state, an electron is promoted from the  $1a_2$  orbital to the  $3b_1$  orbital.

$$^2A_2: (\text{core}) (5a_1)^2(3b_2)^2(6a_1)^2(7a_1)^2 \\ (4b_2)^2(2b_1)^2(5b_2)^2(8a_1)^2(1a_2)^1(3b_1)^2.$$

For the  $^2A_1$  excited state, an electron is promoted from the  $8a_1$  orbital to the  $3b_1$  orbital.

$$^2A_1: (\text{core}) (5a_1)^2(3b_2)^2(6a_1)^2(7a_1)^2 \\ (4b_2)^2(2b_1)^2(5b_2)^2(8a_1)^1(1a_2)^2(3b_1)^2.$$

And finally, for the  $^2B_2$  excited state, an electron is promoted from the  $5b_2$  orbital to the  $3b_1$  orbital.

$$^2B_2: (\text{core}) (5a_1)^2(3b_2)^2(6a_1)^2(7a_1)^2 \\ (4b_2)^2(2b_1)^2(5b_2)^1(8a_1)^2(1a_2)^2(3b_1)^2.$$

Of the three transitions, ( $^2A_2 \leftarrow ^2B_1$ ,  $^2A_1 \leftarrow ^2B_1$ ,  $^2B_2 \leftarrow ^2B_1$ ), only the first ( $^2A_2 \leftarrow ^2B_1$ ) has been de-

tected experimentally. The  ${}^2B_2$  transition is not dipole allowed from the ground state while the  ${}^2A_1$  transition is predicted to be much weaker and overlapping with the  ${}^2A_2$  transition.

The vibrational structure of the A  ${}^2A_2$  band is dominated by a long progression in  $\nu_1$  with shorter associated progressions in  $\nu_2$  and even quanta of  $\nu_3$ . Since the asymmetric transition ( $2\nu_3$ ) is not allowed assuming the same symmetry ( $C_{2v}$ ) for both electronic states and assuming only a harmonic oscillator function, the  $2\nu_3$  intensities are believed to result either from a double minimum in the  $\nu_3$  potential function (unequal excited state Cl–O bond lengths) or from non-harmonic (higher-order) coupling between even levels of  $\nu_3$  and the allowed  $\nu_1$  and  $\nu_2$  transitions. Although there is no doubt that this effect is occurring, there is some ambiguity in the literature as to which explanation is the more appropriate [18,20–22].

The most definitive work to date in analyzing the A  ${}^2A_2$  vibrational structure has been by Vaida and co-workers, using a novel technique combining a supersonic molecular jet with a high-resolution Fourier transform ultraviolet spectrometer [22–24]. Vibronic linewidths are found to increase uniformly with energy such that lifetimes decrease from about 100 ps at 435 nm to about 1 ps at 303 nm. Since asymmetric stretch and bend vibrations show short lifetimes even at low energy, it can be concluded that both  $\nu_2$  and  $\nu_3$  modes are involved in photodissociation and/or photoisomerization. The low rotational temperatures ( $\approx 30$ – $80$  K) present in the molecular jet also enable an approximate measurement of the Cl–O bond length (1.645 Å) and bond angle ( $104.5^\circ$ ) for the A  ${}^2A_2$  electronic state. Harmonic frequencies for  ${}^{35}\text{Cl}$  for the  ${}^2A_2 \leftarrow {}^2B_1$  transition were found to be

$$\omega_1^0 = 705.9 \text{ cm}^{-1}, \quad \omega_2^0 = 284.2 \text{ cm}^{-1},$$

$$\text{and } 2\omega_3^0 = 821.6 \text{ cm}^{-1}.$$

Finally, the most quantitative work to date in terms of absolute photoabsorption cross sections for the  ${}^2A_2$  transition has been by Wahner, Tyndall, and Ravishankara using a xenon lamp and a diode array detector [25]. They measured absolute cross sections based on OCIO partial pressures and by reacting OCIO with NO to produce  $\text{NO}_2$ . OCIO absorption was found to be linear up to an optical density of 1 after

which non-Beers law behavior was observed. Bands were found to become sharper and the underlying continuum weaker as the absorption cell temperature was lowered from 378 to 296 to 204 K.

Unfortunately, the upper electronic states of  $\text{ClO}_2$  have not been studied as extensively experimentally or theoretically (the  ${}^4B_2$  quartet state has been predicted to lie near the first vacuum UV band at 183 nm [18]). Photoelectron spectra provide the most extensive expansion into the vacuum UV [19,26]. Although the first three ionization potentials are well established, there appears to be some uncertainty as to the location of the fourth ionization potential (possibly due to a lower instrument resolution in the earlier work)

$$\text{IP}_1 = 10.35 \text{ eV} = 83468 \text{ cm}^{-1},$$

$$\text{IP}_2 = 12.40 \text{ eV} = 100000 \text{ cm}^{-1},$$

$$\text{IP}_3 = 15.25 \text{ eV} = 122984 \text{ cm}^{-1}.$$

Vibrational structure consistent with the ground state vibrational frequencies can also be seen for the first three ionization bands as expected for the removal of an electron from a weakly anti-bonding orbital ( $3b_1$ ).

The photoabsorption spectrum for  $\text{ClO}_2$  in the vacuum UV was first studied by Humphries et al. [27]. They found a small number of vibrational band progressions superimposed on a rapidly rising continuum. The first two band groups were assigned to a Rydberg progression leading to the first ionization potential while the third was assigned to another Rydberg progression leading to the second ionization potential. Subsequently, Basco and Morse [28] confirmed most of Humphries' peak locations and reported approximate extinction coefficients for the more prominent bands. In neither case were electronic states definitively established and vibrational progressions were only vaguely assigned. More recently, Baumgartel and co-workers [19] reported absorption spectra in the vacuum UV and assigned most of the bands to a Rydberg progression leading to the first ionization potential involving  $ns$ ,  $np_z$ ,  $np_x$ , and  $nd$  Rydberg orbitals. In the present work, we report absolute photoabsorption cross sections for  $\text{ClO}_2$  at room temperature between 125 and 470 nm and discuss the electronic spectrum of  $\text{ClO}_2$  in the vacuum UV.

## 2. Experimental

Fresh samples of  $\text{ClO}_2$  were prepared by flowing  $\text{Cl}_2$  (Matheson, UHP) through a column of  $\text{NaClO}_2$ . Initially, affluent from the  $\text{NaClO}_2$  column was used directly without further purification or storage. However, it was found that peak cross sections were unreliable and varied by approximately a factor 2 from experiment to experiment. The most reliable method found was to trap dry  $\text{ClO}_2$  at dry ice temperature ( $-78^\circ\text{C}$ ) after drying with  $\text{P}_2\text{O}_5$ . The dry  $\text{ClO}_2$  was then allowed to warm up until the pressure in a 15 l tank system reached 50 to 100 Torr. Argon was then added until a final pressure of 300 to 600 Torr was reached. Mixtures containing between 5% and 40%  $\text{ClO}_2$  were then used for a day's experiment. Although samples of  $\text{ClO}_2/\text{Ar}$  were safely stored at room temperature for periods of up to 48 h, longer storage periods resulted in *an explosive mixture which would detonate if touched*. It was also found that cross sections were more reliable if the  $\text{ClO}_2/\text{Ar}$  was used immediately and hence, in all subsequent experiments, spectral measurements were made immediately after  $\text{ClO}_2$  preparation. Typically, sample and background pressures were  $\approx 1$  Torr and were then subtracted to determine the real  $\text{ClO}_2/\text{Ar}$  pressure.  $\text{ClO}_2$  partial pressures were then used to determine absolute cross sections.

The optical system used consisted of a Minuteman 0.5 m vacuum monochrometer with a dispersion of 1.67 nm/mm driven electronically by an IBM PC computer, a pyrex flow cell and vacuum manifold with a total path length of either 14.0, 73.0 or 110.0 cm, a Hamamatsu deuterium lamp (L1626 and L879) or a krypton microwave discharge continuum light source and a Hamamatsu photomultiplier sensitive either in the UV/near UV (1P28) or in the vacuum UV (CsTe R1460, CsI R1459). Signals from the PMT were detected with a pulse discriminator and amplifier system and then recorded by an IBM PC computer using an analog to digital converter. Wavelength data along with the signal from the PMT were recorded to disk simultaneously by an in-house C program. Recorded wavelengths were periodically recalibrated with a low-pressure Hg lamp.

Since an original goal of this work was to determine absolute cross sections in the vacuum UV as a function of temperature, flow cell and vacuum man-

ifold temperatures were maintained to within  $0.1^\circ\text{C}$  using fiberglass and styrofoam isolation and a constant temperature flow bath ( $-30$  to  $30^\circ\text{C}$ ). Flow cell and vacuum manifold temperatures were measured with a digital thermometer. However, it was found that experimental error greatly overwhelmed any expected temperature effect (10% to 20%) and thus, all subsequent experiments were done at  $25^\circ\text{C}$ .

Finally, individual experiments for each spectral region were averaged as cross sections and then combined into one file. Only spectra with absorbances below 1.0 were used in this averaging process in order to prevent saturation effects. Averages for each spectral region (determined by intensity of light source) were combined into one file by starting at the long wavelength region (300 to 400 nm), which could be calibrated using the data of Wahner et al., and then adjusting each file so that a smooth transition was observed from region to region. All adjustments were less than 25% and were usually zero. For the data overall (125 to 470 nm), cross section precision was on the order of  $\pm 10\%$ .

## 3. Results and discussion

Although isolated portions of the absorption spectrum for  $\text{ClO}_2$  have been reported, most notably by Wahner et al. in the near UV and by Basco and Morse, and Humphries et al. in the vacuum UV, this work allowed us to record the entire spectrum for  $\text{ClO}_2$  between 125 and 470 nm. In fig. 1, at least four separate band systems can be seen ( $A^2A_2$ , C, D/E, F). Upon scale expansion, the D and E systems are found to represent separate progressions.

Our cross sections for the symmetric stretch bands ( $\nu_{n,0,0}$ ,  $n=2$  to  $n=26$ ) are consistent with those reported by Wahner et al. at room temperature ( $\pm 9\%$  overall,  $+4\%$  on average) with deviations increasing for low and high vibrations where both their data and our data are more uncertain ( $\approx \pm 20\%$ ). Cross sections for the combination bands  $\nu_{n,1,0}$ ,  $\nu_{n,0,2}$ , and  $\nu_{n,1,2}$  have not been reported previously but are believed to be reliable to within 10%. The only tabulated cross sectional data for the vacuum UV region are by Basco and Morse. Although cross sections for the few peaks reported are roughly consistent with our data, significant deviations do occur (up to  $\pm 50\%$ ) for the C,

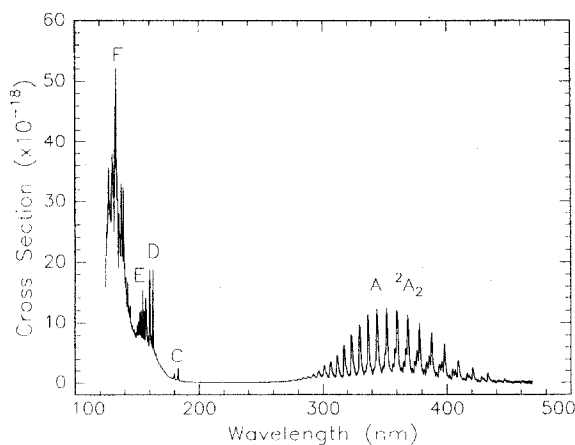


Fig. 1. The absorption spectrum of  $\text{ClO}_2$  at room temperature.

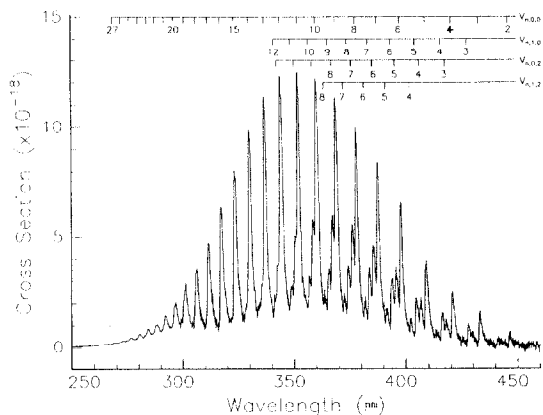


Fig. 2. The photoabsorption spectrum of the  $A^2A_2$  system.

D, and E systems. Cross sections for the F system were not reported. Although individual values were not tabulated, Baumgartel and co-workers also report cross sections consistent with our data except for slightly lower values in the F region as indicated in fig. 5 of ref. [19].

### 3.1. UV region

Four different band progressions can be identified in the  $A^2A_2$  system (fig. 2). Following Vaida et al., they are identified as (1) a progression in symmetrical stretch ( $\nu_{n,0,0}$ ) starting with  $n=2$  to  $n=27$ ; (2) a progression in symmetrical stretch plus one quanta

of bending vibration ( $\nu_{n,1,0}$ ) starting at  $n=3$  to  $n=12$ ; (3) a progression in symmetric stretch plus two quanta of asymmetric stretch ( $\nu_{n,0,2}$ ) starting at  $n=3$  to  $n=11$ ; and (4) a progression in symmetric stretch plus one quanta of bending vibration and two quanta of asymmetric stretch ( $\nu_{n,1,2}$ ). The major uncertainty in determining these bands was our inability to uniquely assign the band head for each peak. Band heads were fixed at the leading edge (high energy) of each absorption peak. While this worked well on the larger peaks, it did not work very well on the smaller peaks and resulted in a band head uncertainty of  $\approx 10 \text{ cm}^{-1}$ . Nevertheless, we are able to report good cross sectional data for 26 primary bands ( $\nu_{n,0,0}$ ) and 24 combination bands ( $\nu_{n,1,0}$ ,  $\nu_{n,0,2}$  and  $\nu_{n,1,2}$ ) of the  $A^2A_2$  transition (table 1). Although our wavelength positions are not as precise as those by Vaida et al., our data clearly show the expected trends in  $\nu_{n,0,0}$ ,  $\nu_{n,1,0}$ ,  $\nu_{n,0,2}$  and  $\nu_{n,1,2}$  and are consistent with reported vibrational frequencies and anharmonicities.

Vibrational analysis of the  $A^2A_2$  band system yielded vibrational parameters very close to those found by Vaida et al. [23] for  $^{35}\text{Cl}$ . The symmetric stretch frequency ( $\omega_1^0$ ) was found to be  $735 \pm 10 \text{ cm}^{-1}$  with an anharmonicity constant ( $X_{11}$ ) equal to  $-4.9 \pm 0.3$ . Thus, the fundamental frequency  $\nu_1$  was found to be  $731 \text{ cm}^{-1}$ . Although determination of the zero-point energy  $\nu_{0,0,0}$  is less accurate due to extrapolation errors, we estimate  $\nu_{0,0,0}$  to be at  $20962 \text{ cm}^{-1}$ . Likewise, the bending frequency ( $\omega_2^0$ ) was found to be  $291 \pm 6 \text{ cm}^{-1}$  with an anharmonicity constant ( $X_{12}$ ) equal to  $-3.9 \pm 0.7$  and the asymmetric stretching frequency ( $2\omega_3^0$ ) was found to be  $866 \pm 5 \text{ cm}^{-1}$  with an anharmonicity constant ( $X_{13}$ ) equal to  $-5.0 \pm 0.4$ . Since progressions in  $\nu_1$  only were observed, the other anharmonicity constants ( $X_{22}$ ,  $X_{23}$ ,  $X_{33}$ ) could not be evaluated accurately and hence the given values for  $\omega_2^0$  and  $2\omega_3^0$  include minor contributions due to  $X_{22}$  and  $X_{33}$  respectively. Using these vibrational parameters, we have extrapolated our cross sectional data down to  $\nu_{0,0,0}$  for each vibrational mode (table 2). Cross sections were estimated for  $\nu_{0,0,0}$ ,  $\nu_{1,0,0}$ ,  $\nu_{0,1,0}$ ,  $\nu_{1,1,0}$ ,  $\nu_{2,1,0}$ ,  $\nu_{0,0,2}$ ,  $\nu_{1,0,2}$ , and  $\nu_{2,0,2}$  by extrapolating each progression set to  $\nu_0$  by hand while maintaining the approximate curvature of the known cross sections. For the combination bands  $\nu_{n,1,2}$ , insufficient data was available for this procedure and hence no extrapolation was attempted.

Table 1

Band	Wavelength (nm) band head	Frequency ( $\text{cm}^{-1}$ )	Cross section	$\nu_{n+1} - \nu_n$
<b>A<sup>2</sup>A<sub>2</sub> system – symmetric stretch</b>				
$\nu_{2,0,0}$	446.17	22413	$0.76 \times 10^{-18}$	694
$\nu_{3,0,0}$	432.78	23107	$1.70 \times 10^{-18}$	680
$\nu_{4,0,0}$	420.40	23787	$2.57 \times 10^{-18}$	677
$\nu_{5,0,0}$	408.77	24464	$3.93 \times 10^{-18}$	681
$\nu_{6,0,0}$	397.69	25145	$6.60 \times 10^{-18}$	666
$\nu_{7,0,0}$	387.43	25811	$8.43 \times 10^{-18}$	668
$\nu_{8,0,0}$	377.65	26479	$10.00 \times 10^{-18}$	663
$\nu_{9,0,0}$	368.43	27142	$11.40 \times 10^{-18}$	652
$\nu_{10,0,0}$	359.80	27794	$12.21 \times 10^{-18}$	642
$\nu_{11,0,0}$	351.67	28436	$12.51 \times 10^{-18}$	653
$\nu_{12,0,0}$	343.78	29089	$12.31 \times 10^{-18}$	614
$\nu_{13,0,0}$	336.66	29703	$11.41 \times 10^{-18}$	631
$\nu_{14,0,0}$	329.66	30334	$9.91 \times 10^{-18}$	620
$\nu_{15,0,0}$	323.06	30954	$8.10 \times 10^{-18}$	599
$\nu_{16,0,0}$	316.93	31553	$6.40 \times 10^{-18}$	562
$\nu_{17,0,0}$	311.38	32115	$4.75 \times 10^{-18}$	572
$\nu_{18,0,0}$	305.93	32687	$3.62 \times 10^{-18}$	549
$\nu_{19,0,0}$	300.88	33236	$2.92 \times 10^{-18}$	548
$\nu_{20,0,0}$	296.00	33784	$2.07 \times 10^{-18}$	492
$\nu_{21,0,0}$	291.75	34276	$1.46 \times 10^{-18}$	507
$\nu_{22,0,0}$	287.50	34783	$1.08 \times 10^{-18}$	442
$\nu_{23,0,0}$	283.89	35225	$0.89 \times 10^{-18}$	505
$\nu_{24,0,0}$	279.88	35730	$0.65 \times 10^{-18}$	498
$\nu_{25,0,0}$	276.03	36228	$0.47 \times 10^{-18}$	516
$\nu_{26,0,0}$	272.15	36744	$0.30 \times 10^{-18}$	497
$\nu_{27,0,0}$	268.52	37241	$0.22 \times 10^{-18}$	
<b>A<sup>2</sup>A<sub>2</sub> system – bend</b>				
$\nu_{3,1,0}$	427.58	23387	$1.13 \times 10^{-18}$	671
$\nu_{4,1,0}$	415.66	24058	$1.61 \times 10^{-18}$	674
$\nu_{5,1,0}$	404.33	24732	$2.26 \times 10^{-18}$	681
$\nu_{6,1,0}$	393.50	25413	$3.13 \times 10^{-18}$	669
$\nu_{7,1,0}$	383.40	26082	$3.64 \times 10^{-18}$	661
$\nu_{8,1,0}$	373.93	26743	$3.72 \times 10^{-18}$	652
$\nu_{9,1,0}$	365.03	27395	$3.62 \times 10^{-18}$	643
$\nu_{10,1,0}$	356.66	28038	$3.25 \times 10^{-18}$	656
$\nu_{11,1,0}$	348.50	28694	$2.85 \times 10^{-18}$	632
$\nu_{12,1,0}$	341.00	29326	$2.41 \times 10^{-18}$	
<b>A<sup>2</sup>A<sub>2</sub> system – asymmetric stretch</b>				
$\nu_{3,0,2}$	417.67	23943	$1.32 \times 10^{-18}$	674
$\nu_{4,0,2}$	406.22	24617	$2.29 \times 10^{-18}$	667
$\nu_{5,0,2}$	395.50	25284	$3.70 \times 10^{-18}$	665
$\nu_{6,0,2}$	385.38	35949	$4.65 \times 10^{-18}$	654
$\nu_{7,0,2}$	375.90	26603	$5.62 \times 10^{-18}$	656
$\nu_{8,0,2}$	366.85	27259	$6.01 \times 10^{-18}$	655
$\nu_{9,0,2}$	358.24	27914	$5.84 \times 10^{-18}$	640
$\nu_{10,0,2}$	350.22	38554	$5.08 \times 10^{-18}$	647
$\nu_{11,0,2}$	342.46	29201	$3.70 \times 10^{-18}$	
<b>A<sup>2</sup>A<sub>2</sub> system – asymmetric stretch and bend</b>				
$\nu_{4,1,2}$	401.89	24882	$1.39 \times 10^{-18}$	674
$\nu_{5,1,2}$	391.30	25556	$1.82 \times 10^{-18}$	649
$\nu_{6,1,2}$	381.61	26205	$2.31 \times 10^{-18}$	669
$\nu_{7,1,2}$	372.11	26874	$2.46 \times 10^{-18}$	646
$\nu_{8,1,2}$	363.38	27520	$2.64 \times 10^{-18}$	

Table 2  
Estimated cross sections for low vibrations of the  $A^2A_2$  system

Band	Wavelength (nm)	Frequency ( $\text{cm}^{-1}$ )	Cross section
$\nu_{0,0,0}$	477.05	20962	$0.04 \times 10^{-18}$
$\nu_{1,0,0}$	460.98	21693	$0.24 \times 10^{-18}$
$\nu_{0,1,0}$	470.52	21253	$0.32 \times 10^{-18}$
$\nu_{1,1,0}$	454.96	21980	$0.54 \times 10^{-18}$
$\nu_{2,1,0}$	440.61	22696	$0.80 \times 10^{-18}$
$\nu_{0,0,2}$	458.13	21828	$0.01 \times 10^{-18}$
$\nu_{1,0,2}$	443.48	22549	$0.08 \times 10^{-18}$
$\nu_{2,0,2}$	429.94	23259	$0.60 \times 10^{-18}$

### 3.2. Low absorbance region

We were surprised to find that cross sections between 268.5 nm (last  $A^2A_2$  band) and 183.1 nm (first vacuum UV band) did not go to zero. Although experiments were difficult in this region due to the small cross sectional values, fig. 3a clearly shows a significant cross section ( $4.2 \times 10^{-20}$ ) at 248.4 nm at or near the minimum. Movement away from the minimum to 200.0 nm (fig. 3b) and to 265.0 nm (fig. 3d) re-

sulted in much better fits as absorbances and cross sections increased. We were particularly interested to find non-zero cross sections at 193 nm (fig. 3c) and at 248.4 nm (fig. 3a) as these correspond to excimer laser emissions for ArF and KrF respectively. We believe that these small cross sections result from unresolved high rotational and vibrational lines of the  $^2A_2$  state as suggested by Wahner et al. However, a significant contribution by the underlying  $^2A_1$  state cannot be ruled out.

### 3.3. Vacuum UV region

Like Basco and Morse, and Humphries et al., we find a 3-band system beginning at 183.08 nm which we label as  $C_1$ ,  $C_2$  and  $C_3$  (fig. 4). Vibrational analysis of the C systems is not as exact as in the  $A^2A_2$  system, but, nevertheless, approximate vibrational parameters can still be determined. The C system is dominated by a fundamental vibration at  $C_1$  ( $\nu_0$ ) followed by progressively weaker bands at  $C_2$  ( $\Delta\nu = 981 \text{ cm}^{-1}$ ) and at  $C_3$  ( $\Delta\nu = 969 \text{ cm}^{-1}$ ) (table 3) until the progression is lost beneath a rising continuum after  $C_3$ . This gives an approximate symmet-

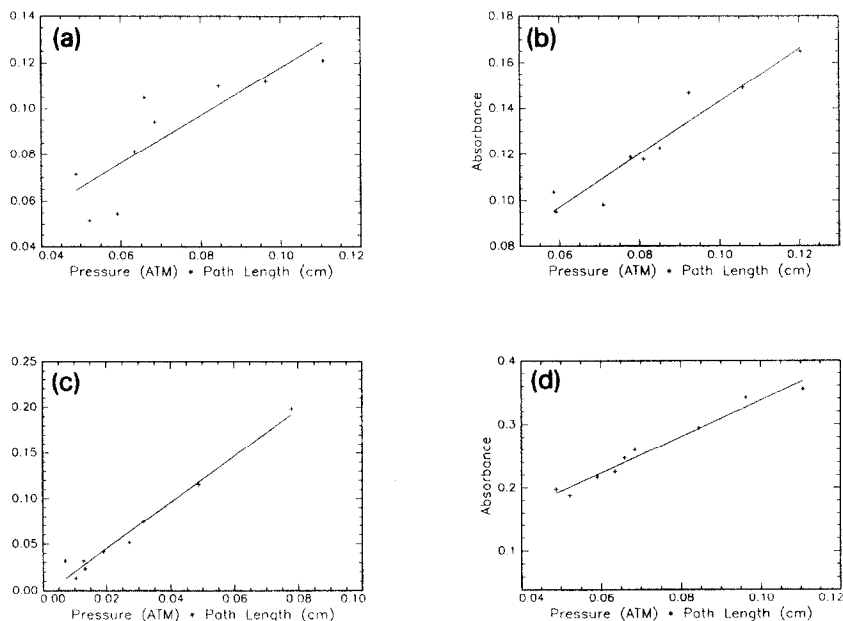


Fig. 3. (a)  $\lambda = 248.4 \text{ nm}$ ,  $\sigma = 0.042 (\pm 0.01) \times 10^{-18}$ . (b)  $\lambda = 200.0 \text{ nm}$ ,  $\sigma = 0.047 (\pm 0.006) \times 10^{-18}$ . (c)  $\lambda = 193.0 \text{ nm}$ ,  $\sigma = 0.103 (\pm 0.006) \times 10^{-18}$ . (d)  $\lambda = 265.0 \text{ nm}$ ,  $\sigma = 0.116 (\pm 0.008) \times 10^{-18}$ .

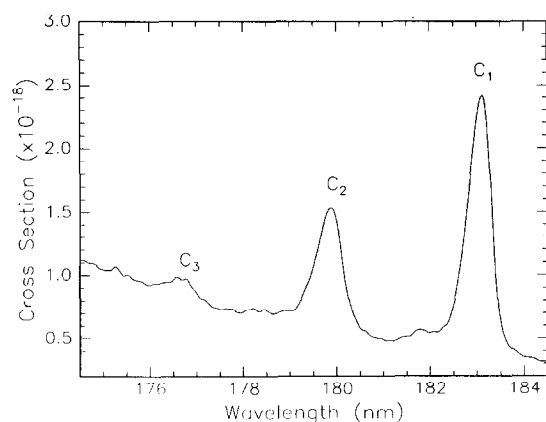


Fig. 4. The photoabsorption spectrum of the C system.

ric stretching frequency of  $975\text{ cm}^{-1}$ . A much weaker (but reproducible) progression in  $\nu_2$  is barely discernable to the blue of each major peak ( $C_1$  and  $C_2$ ) and gives an approximate bending frequency of  $440\text{ cm}^{-1}$ . The consistency of these frequency values with those for the ground state ( $\nu_1'' = 962.8\text{ cm}^{-1}$ ,  $\nu_2'' = 455.4\text{ cm}^{-1}$ ) along with the dominance of the fundamental band  $C_1$  indicates little change in molecular structure. Thus, we can conclude that the C state has a slightly shorter Cl–O bond length and a slightly greater O–C'–O bond angle compared to the ground state.

The next series of bands (D, E) are more complicated because they overlap to a considerable extent and because the D system appears to be composed of three diverging progressions in  $\nu_1$ ,  $\nu_2$ , and  $\nu_3$ . The D system (fig. 5), begins at  $162.66\text{ nm}$  with a primary peak labeled  $D_{0,0,0}$ . However, it is impossible to assign peaks  $D_{0,0,0}$ ,  $D_{1,0,0}$ ,  $D_{0,0,2}$ , and  $D_{0,0,3}$  as one progression. This would result in a widely varying value for  $\nu_{n+1} - \nu_n$  (table 4). It is our conclusion that two progressions are being observed here. At  $D_{1,0,0}$ , there

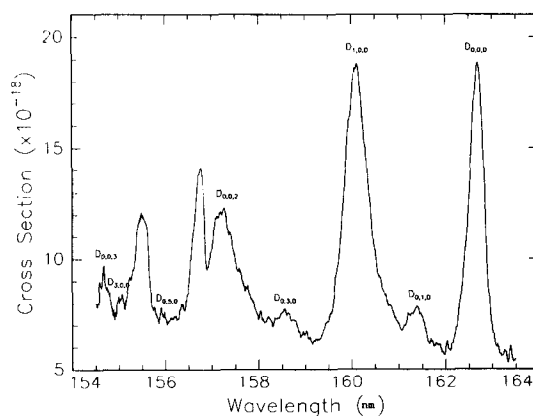


Fig. 5. The photoabsorption spectrum of the D system.

is little difference between the two diverging bands  $\nu_1$  and  $\nu_3$  (symmetrical and asymmetrical stretching respectively). By  $D_{0,0,2}$ , the asymmetric band has become dominant and the symmetric band is a poorly resolved shoulder on the  $D_{0,0,2}$  band. By  $D_{3,0,0}$ , the two progressions have become resolvable as  $D_{3,0,0}$  and  $D_{0,0,3}$ . Following this assumption, two progressional frequencies are detectable,  $992$  and  $1065\text{ cm}^{-1}$  for the symmetric and asymmetric stretching vibrations, respectively, and is again consistent with the ground state parameters ( $962$  and  $1128\text{ cm}^{-1}$ ). A third progression in  $\nu_2$  is also observed at  $D_{0,1,0}$ ,  $D_{0,3,0}$ , and  $D_{0,5,0}$ . This progression is labeled as an independent progression in  $\nu_2$  because the  $D_{1,0,0}$  and  $D_{0,0,2}$  bands are broader than would be expected based on just progressions in  $\nu_1$  and  $\nu_3$ . Unlike the stretching frequencies, the bending progression frequency is significantly larger than the ground state value (22%).

The E system (fig. 6) is very different from the C and D systems in the complete lack of progressions in either  $\nu_1$  or  $\nu_3$  and in the orderliness of the progression in  $\nu_2$  (table 5). Although an exact band origin

Table 3

Band	Wavelength (nm) band head	Frequency ( $\text{cm}^{-1}$ )	Cross section	$\nu_{n+1} - \nu_n$
C system – symmetric stretch				
$C_1$	183.08	54621	$2.42 \times 10^{-18}$	981
$C_2$	179.85	55602	$1.54 \times 10^{-18}$	969
$C_3$	176.77	56571	$0.90 \times 10^{-18}$	

Table 4 <sup>a)</sup>

Band	Wavelength (nm) band head	Frequency (cm <sup>-1</sup> )	Cross section	$\nu_{n+1} - \nu_n$
<b>D system – symmetric stretch</b>				
D <sub>0,0,0</sub>	162.66	61477	18.87 × 10 <sup>-18</sup>	992
D <sub>1,0,0</sub>	160.08	62469	18.85 × 10 <sup>-18</sup>	
D <sub>2,0,0</sub>	(157.58)	(63461)		
D <sub>3,0,0</sub>	155.01	64511	8.71 × 10 <sup>-18</sup>	
<b>D system – asymmetric stretch</b>				
D <sub>0,0,1</sub>	(159.95)	(62520)		1065
D <sub>0,0,2</sub>	157.27	63585	12.34 × 10 <sup>-18</sup>	
D <sub>0,0,3</sub>	154.68	64650	9.72 × 10 <sup>-18</sup>	
Band	Wavelength (nm) band head	Frequency (cm <sup>-1</sup> )	Cross section	$\frac{1}{2}(\nu_{n+2} - \nu_n)$
<b>D system – bending</b>				
D <sub>0,1,0</sub>	161.38	61967	7.88 × 10 <sup>-18</sup>	552
D <sub>0,3,0</sub>	158.55	63070	7.75 × 10 <sup>-18</sup>	536
D <sub>0,5,0</sub>	155.90	64142	7.65 × 10 <sup>-18</sup>	

<sup>a)</sup> Values in parentheses are estimated from  $\nu_{n+1} - \nu_n$ .

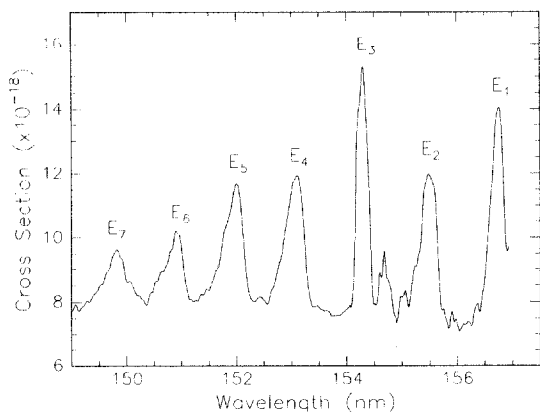


Fig. 6. The photoabsorption spectrum of the E system.

could not be determined due to overlap with the D system, the measured vibrational frequency ( $\omega_2^0$ ) of  $527 \pm 8$  cm<sup>-1</sup> and anharmonicity constant of  $-4.5 \pm 1.0$  was again at least roughly consistent with the ground state but now indicates substantial change in O–Cl–O bond angle and relatively little change in Cl–O bond length in the E state compared to the ground state. Another intriguing possibility is that predissociation may be occurring via the Cl+O<sub>2</sub> path as has been suggested for bending progressions of the

A<sup>2</sup>A<sub>2</sub> state [18,20].

Although the F system (fig. 7) is listed as one system, (primarily for graphical and notational convenience), it is in all probability more than one (as will be discussed later). Frequency spacing overall is  $\approx 500$  cm<sup>-1</sup> (i.e. bending vibration) but varies by as much as 400 cm<sup>-1</sup> on occasion (F<sub>18</sub> to F<sub>19</sub>) (table 6). Analysis is further complicated by peaks which may be due to molecular chlorine (e.g. F<sub>13</sub>, also present in ref. [19]). Nevertheless, the major pattern of vibrational spacing must result from bending progressions (or perhaps overlapping stretching progressions) of two or more excited states.

Humphries et al. labeled band systems C and D as members of a Rydberg progression leading to the first ionization potential. Vibrational spacings are similar to ground state values as expected for a Rydberg transition where an electron is removed from the antibonding  $b_1 - \pi_u^*$  molecular orbital. Humphries et al. also reported molecular orbital calculations which showed that removal of an electron from the  $b_1 - \pi_u^*$  would have little or no effect on the OClO bond angle in accordance with the lack of or diminished importance of bending progressions in the C and D systems. Thus, the first two Rydberg orbitals can be safely designated as  $sa_1$  (4s) and as  $pa_1$  (4p<sub>z</sub><sup>o</sup>) in ac-

Table 5

Band	Wavelength (nm) band head	Frequency ( $\text{cm}^{-1}$ )	Cross section	$\nu_{n+1} - \nu_n$
<b>E system – bending</b>				
E <sub>1</sub>	156.75	63798	$14.10 \times 10^{-18}$	519
E <sub>2</sub>	155.48	64317	$12.11 \times 10^{-18}$	494
E <sub>3</sub>	154.30	64811	$15.47 \times 10^{-18}$	504
E <sub>4</sub>	153.11	65315	$11.96 \times 10^{-18}$	479
E <sub>5</sub>	151.99	65794	$11.70 \times 10^{-18}$	477
E <sub>6</sub>	150.90	66271	$10.23 \times 10^{-18}$	471
E <sub>7</sub>	149.83	66742	$9.65 \times 10^{-18}$	

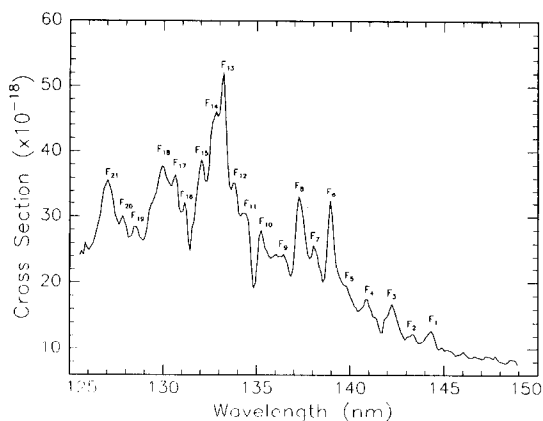


Fig. 7. The photoabsorption spectrum of the F system.

cordance with Humphries and should result in transitions which are perpendicular in type.

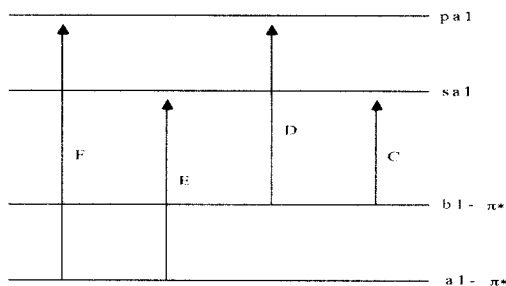
The E and F systems are substantially different from the C and D systems. Progressions in  $\nu_1$  and  $\nu_3$  are not detected. The first band is not the largest band and indicates considerable change in nuclear parameters (primarily in OCIO bond angle). For these reasons, Humphries et al. assigned the E system to a Rydberg progression leading to the second ionization potential. Both the E and the F systems are consistent with a Rydberg progression where an electron from the anti-bonding  $a_1 - \pi_u^*$  orbital is promoted to the same Rydberg orbitals as found in the C and D systems (i.e.  $sa_1$  and  $pa_1$ ). Since the anti-bonding nature of the  $a_1 - \pi_u^*$  orbital is partly relieved by bending, promotion of an electron from this orbital should result in a considerable increase in OCIO bond angle and therefore result in a large progression in  $\nu_2$  as observed for the E and F systems.

There is one flaw in this reasoning. If the E and F systems have the same final orbital as the C and D systems ( $sa_1$  and  $pa_1$ , respectively), we should be able to predict the energy difference between the two ground state orbitals  $a_1 - \pi_u^*$  and  $b_1 - \pi_u^*$  by comparing bands C<sub>1</sub> and D<sub>1</sub> versus bands E<sub>1</sub> and F<sub>1</sub>. In other words, absorptions in the C system result from the promotion of an electron from the  $b_1 - \pi_u^*$  orbital to the  $sa_1$  Rydberg orbital, absorptions in the D system result from the promotion of an electron from the  $b_1 - \pi_u^*$  orbital to the  $pa_1$  Rydberg orbital, absorptions in the E system result from the promotion of an electron from the  $a_1 - \pi_u^*$  orbital to the  $sa_1$  Rydberg orbital, and finally, absorptions in the F system result from the promotion of an electron from the  $a_1 - \pi_u^*$  orbital to the  $pa_1$  Rydberg orbital (see scheme 1).

This comparison predicts that there should be an intervalence transfer band ( ${}^2A_1 \leftarrow {}^2B_1$ ) somewhere between  $7829 \text{ cm}^{-1}$  ( $F_1 - D_1$ ) and  $9177 \text{ cm}^{-1}$  ( $E_1 - C_1$ ). However, the  ${}^2A_1$  state is predicted [18] to lie much closer to the  ${}^2A_2$  state and should be  $\approx 20000 \text{ cm}^{-1}$  above the  ${}^2B_1$  ground state and not  $\approx 10000 \text{ cm}^{-1}$  as predicted in the above ( $E_1 - C_1$ ). This means that the E state cannot share the same final orbital as in either the C or D transitions. Baumgartel and co-workers [19] have suggested a different band labeling. While they agree that first two band systems (C and D) result from a Rydberg progression leading to the first ionization potential and involve the Rydberg orbitals  $4s$  and  $4p_z^o$ , the E system is also reported to result from a Rydberg progression leading to the first ionization potential and involve the Rydberg orbital  $4p_x^o$ . Baumgartel and co-workers further assigned the peaks shown in fig. 7 to a variety of Rydberg orbitals also leading to the first ionization potential ( $F_1 = 4d$ ,

Table 6

Band	Wavelength (nm) band head	Frequency ( $\text{cm}^{-1}$ )	Cross section	$\nu_{n+1} - \nu_n$
F system - bending				
F <sub>1</sub>	144.29	69306	$12.80 \times 10^{-18}$	484
F <sub>2</sub>	143.29	69790	$12.40 \times 10^{-18}$	550
F <sub>3</sub>	142.17	70340	$16.72 \times 10^{-18}$	649
F <sub>4</sub>	140.87	70989	$17.56 \times 10^{-18}$	553
F <sub>5</sub>	139.78	71542	$19.60 \times 10^{-18}$	400
F <sub>6</sub>	139.00	71942	$32.20 \times 10^{-18}$	522
F <sub>7</sub>	138.00	72464	$25.40 \times 10^{-18}$	399
F <sub>8</sub>	137.24	72863	$33.00 \times 10^{-18}$	547
F <sub>9</sub>	136.22	73410	$24.40 \times 10^{-18}$	542
F <sub>10</sub>	135.22	73952	$28.00 \times 10^{-18}$	458
F <sub>11</sub>	134.38	74410	$30.80 \times 10^{-18}$	310
F <sub>12</sub>	133.83	74720	$35.08 \times 10^{-18}$	355
F <sub>13</sub>	133.20	75075	$52.00 \times 10^{-18}$	239
F <sub>14</sub>	132.78	75314	$46.00 \times 10^{-18}$	411
F <sub>15</sub>	132.06	75725	$38.60 \times 10^{-18}$	533
F <sub>16</sub>	131.13	76258	$28.40 \times 10^{-18}$	303
F <sub>17</sub>	130.61	76561	$33.60 \times 10^{-18}$	362
F <sub>18</sub>	130.00	76923	$37.60 \times 10^{-18}$	891
F <sub>19</sub>	128.51	77814	$28.40 \times 10^{-18}$	447
F <sub>20</sub>	127.78	78261	$30.00 \times 10^{-18}$	479
F <sub>21</sub>	127.00	78740	$35.60 \times 10^{-18}$	



Scheme 1.

$F_4 = 5s$ ,  $F_6 = 5p_z^\sigma$ ,  $F_9 = 5p_x^\pi$ ,  $F_{16} = 6s$ ,  $F_{19} = 6p_x^\pi$ ). While we cannot dispute these last assignments (we did not go as far into the vacuum UV as in ref. [19]), our data does not support them either. Conventional wisdom is contradicted to such an extent in terms of the constancy of the quantum defect with  $n$  (quantum defects are shown to actually go up and then down again as  $n$  goes from 4 to 5 to 6) and in terms of the expected decrease in extinction coefficients with  $n$ , that these later assignments are of mostly notational value and have little predictive value. We would like

to suggest a different possibility. The  $^4B_2$  state has been predicted [18] to lie 6.82 eV (181.82 nm) above the  $^2B_1$  ground state. This is almost the exact value for the  $C_1$  transition (183.08 nm). The other three quartet states are also predicted to lie near the E system energy:  $^4A_2$  155.78;  $^4A_1$  153.47; and  $^4B_1$  149.94 nm. Ever since the original work of Humphries et al., the possibility that some of the OCIO vacuum UV transitions might result from electronic and not Rydberg states has been ignored. In light of the closeness of theoretical predictions with at least two of the vacuum UV transitions, we believe that this possibility must be explored further.

#### 4. Conclusion

In the present work we have reported absolute absorption cross sections for OCIO between 125 and 470 nm. In all, cross sections for 26 primary symmetric stretching bands and 24 combination bending and asymmetric stretching bands of the  $A^2A_2$  system were measured between 260 and 460 nm. These bands for

natural abundance OCIO were analyzed in terms of vibrational frequencies  $\omega_1^0$ ,  $\omega_2^0$ , and  $2\omega_3^0$  and anharmonicity constants  $X_{11}$ ,  $X_{12}$ , and  $X_{13}$  and compared to those reported by Vaida et al. for  $^{35}\text{Cl}$ . Four additional band systems in the vacuum UV (C, D, E, F) were also analyzed in order to determine approximate vibrational frequencies and anharmonicity constants. These latter band systems were also discussed in terms of a Rydberg progression leading to the first ionization potential involving the Rydberg orbitals  $ns$ ,  $np_z^{\sigma}$ ,  $np_x^{\pi}$ , and  $nd$  and in terms of possible quartet states in the vacuum UV. Finally, a cross sectional minimum of  $4 \times 10^{-20} \text{ cm}^2 \text{ molecule}^{-1}$  near 248 nm was found between the  $A^2A_2$  system and the C system.

### Acknowledgement

We would like to thank the National Science Council of the Republic of China for their generous support of this work (grant No. NSC83-0208-M008-042) and the National Central University in Chung-Li, Taiwan for the facilities and material support used in this work. Finally, SH would like to thank the National Science Council for his fellowship support (grant No. NSC82-0208-M008-075).

### References

- [1] R.F. Curl Jr., K. Abe, J. Bissinger, C. Bennet and F.K. Tittel, *J. Mol. Spectry.* 48 (1973) 72.
- [2] T. Heiderberg, M. Sugden, D.R. Jenkins and L.N. Kenney, *Phys. Rev.* 121 (1961) 1119.
- [3] R.F. Curl, R.F. Heiderberg and J.L. Kinsey, *Phys. Rev.* 125 (1962) 1993.
- [4] W.M. Tolles, J.L. Kinsey, R.F. Curl Jr. and R.F. Heiderberg, *J. Chem. Phys.* 37 (1962) 927.
- [5] M.G. Krishna Pillai and R.F. Curl Jr., *J. Chem. Phys.* 37 (1962) 2921.
- [6] R.P. Mariella and R.F. Curl Jr., *J. Chem. Phys.* 52 (1970) 757.
- [7] K. Tanaka and T. Tanaka, *J. Mol. Spectry.* 98 (1983) 425.
- [8] J.B. Coon and E. Ortiz, *J. Mol. Spectry.* 1 (1957) 81.
- [9] Y. Hamada and M. Tsuboi, *Bull. Chem. Soc. Japan* 52 (1979) 383.
- [10] H. Jones, *Chem. Phys. Letters* 69 (1980) 483.
- [11] H. Jones, *J. Mol. Struct.* 60 (1980) 215.
- [12] H. Jones and W. Lienert, *Phys. Letters* 73 (1980) 417.
- [13] Y. Hamada and M. Tsuboi, *J. Mol. Spectry.* 83 (1980) 373.
- [14] H. Jones and J.M. Brown, *J. Mol. Spectry.* 90 (1981) 222.
- [15] H. Uehara and K. Hakuta, *J. Chem. Phys.* 74 (1981) 769.
- [16] M. Tanoura, K. Chiba and K. Tanaka, *J. Mol. Spectry.* 95 (1982) 157.
- [17] K. Miyazaki, M. Tanoura, K. Tanaka and T. Tanaka, *J. Mol. Spectry.* 116 (1986) 435.
- [18] K.A. Peterson and H.J. Werner, *J. Chem. Phys.* 96 (1992) 8948.
- [19] R. Flesch, E. Ruhl, K. Hoffmann and H. Baumgartel, *J. Phys. Chem.* 97 (1993) 837.
- [20] E.C. Richard and V. Vaida, *J. Chem. Phys.* 94 (1991) 163.
- [21] J.C.D. Brand, R.W. Redding and A.W. Richardson, *J. Mol. Spectry.* 34 (1970) 399.
- [22] E.C. Richard, C.T. Wickham-Jones and V. Vaida, *J. Phys. Chem.* 93 (1989) 6346.
- [23] E.C. Richard and V. Vaida, *J. Chem. Phys.* 94 (1991) 153.
- [24] V. Vaida, S. Solomon, E.L. Richard, E. Ruhl and A. Jefferson, *Nature* 342 (1989) 405.
- [25] A. Wahner, G.S. Tyndall and A.R. Ravishankara, *J. Phys. Chem.* 91 (1987) 2734.
- [26] A.B. Cornford, D.C. Frost, F.G. Herring and C.A. McDowell, *Chem. Phys. Letters* 10 (1971) 345.
- [27] C.M. Humphries, A.D. Walsh and P.A. Warsop, *Discussions Faraday Soc.* 35 (1963) 137.
- [28] N. Basco and R.D. Morse, *Proc. Roy. Soc. A* 336 (1974) 495.